Video Article

Novel Photoacoustic Microscopy and Optical Coherence Tomography Dual-modality Chorioretinal Imaging in Living Rabbit Eyes

Chao Tian[1], Wei Zhang[2,3], Van Phuc Nguyen[1], Xueding Wang[2,4], Yannis M. Paulus[1,2]

[1]Kellogg Eye Center, Department of Ophthalmology and Visual Sciences, University of Michigan

[2]Department of Biomedical Engineering, University of Michigan

[3]Institute of Biomedical Engineering, Chinese Academy of Medical Sciences & Peking Union Medical College

[4]Department of Radiology, University of Michigan

Correspondence to: Yannis M. Paulus at ypaulus@med.umich.edu

URL: https://www.jove.com/video/57135
DOI: doi:10.3791/57135

Keywords: Engineering, Issue 132, Biomedical engineering, medicine, ophthalmology, photoacoustic imaging, photoacoustic microscopy, optical coherence tomography, ophthalmic optics and devices, chorioretinal imaging, retinal imaging

Date Published: 2/8/2018

Citation: Tian, C., Zhang, W., Nguyen, V.P., Wang, X., Paulus, Y.M. Novel Photoacoustic Microscopy and Optical Coherence Tomography Dual-modality Chorioretinal Imaging in Living Rabbit Eyes. *J. Vis. Exp.* (132), e57135, doi:10.3791/57135 (2018).

Abstract

Photoacoustic ocular imaging is an emerging ophthalmic imaging technology that can noninvasively visualize ocular tissue by converting light energy into sound waves and is currently under intensive investigation. However, most reported work to date is focused on the imaging of the posterior segment of the eyes of small animals, such as rats and mice, which poses challenges for clinical human translation due to small eyeball sizes. This manuscript describes a novel photoacoustic microscopy (PAM) and optical coherence tomography (OCT) dual-modality system for posterior segment imaging of the eyes of larger animals, such as rabbits. The system configuration, system alignment, animal preparation, and dual-modality experimental protocols for *in vivo*, noninvasive, label-free chorioretinal imaging in rabbits are detailed. The effectiveness of the method is demonstrated through representative experimental results, including retinal and choroidal vasculature obtained by the PAM and OCT. This manuscript provides a practical guide to reproducing the imaging results in rabbits and advancing photoacoustic ocular imaging in larger animals.

Video Link

The video component of this article can be found at https://www.jove.com/video/57135/

Introduction

Recent decades have witnessed the explosive development of the field of biomedical photoacoustic imaging[1,2,3,4,5,6,7,8]. Based on the energy conversion of light into sound, the emerging photoacoustic imaging can visualize biological samples at scales from organelles, cells, tissues, organs to small-animal whole body and can reveal its anatomical, functional, molecular, genetic, and metabolic information[1,2,9,10,11,12]. Photoacoustic imaging has found unique applications in a range of biomedical fields, such as cell biology[13,14], vascular biology[15,16], neurology[17,18], oncology[19,20,21,22], dermatology[23], pharmacology[24], and hematology[25,26]. Its application in ophthalmology, that is, photoacoustic ocular imaging, has attracted substantial interests from both scientists and clinicians and is currently under active investigation.

In contrast to routinely used ocular imaging technologies[27], such as fluorescein angiography (FA) and indocyanine green angiography (ICGA) (based on fluorescence contrast), optical coherence tomography (OCT) (based on optical scattering contrast), and its derivative OCT angiography (based on motion contrast of red blood cells), photoacoustic ocular imaging uses optical absorption as the contrast mechanism. This is different from conventional ocular imaging technologies and provides a unique tool for studying optical absorption properties of the eye, which are usually associated with the pathophysiological status of ocular tissue[28]. To date, significant excellent work has been done in photoacoustic ocular imaging[29,30,31,32,33,34,35,36,37], but these studies focus on the posterior segment of the eyes of small animals, such as rats and mice. The pioneering studies well demonstrate the feasibility of photoacoustic imaging in ophthalmology but there is still a long way to go towards clinical translation of the technology since eyeball sizes of rats and mice are much smaller (less than one-third) than that of humans. Due to the propagation of ultrasound waves over a significantly longer distances, signal intensity and image quality may greatly suffer when the technique is used for imaging the posterior segment of larger eyes.

Towards this goal, we recently reported the noninvasive, label-free chorioretinal imaging in living rabbits using integrated photoacoustic microscopy (PAM) and spectral-domain OCT (SD-OCT)[38]. The system has excellent performance and could visualize the retina and choroid of the eyes of larger animals based on endogenous absorption and scattering contrast of ocular tissue. Preliminary results in rabbits show that the PAM could noninvasively distinguish individual retinal and choroidal blood vessels using a laser exposure dose (~80 nJ) significantly below the American National Standards Institute (ANSI) safety limit (160 nJ) at 570 nm[39]; and the OCT could clearly resolve different retinal layers, the choroid, and the sclera. It is the very first demonstration of posterior segment imaging of larger animals using PAM and might be a major step

towards clinical translation of the technology considering that the eyeball size of rabbits (18.1 mm)[40] is almost 80% of the axial length of humans (23.9 mm).

In this work, we provide a detailed description of the dual-modality imaging system and experimental protocols used for noninvasive, label-free chorioretinal imaging in living rabbits and demonstrate the system performance through representative retinal and choroidal imaging results.

Protocol

Rabbits are a United States Department of Agriculture (USDA) covered species. Its use in biomedical research needs to follow strict regulations. All rabbit experiments were performed in accordance with the ARVO (The Association for Research in Vision and Ophthalmology) Statement for the Use of Animals in Ophthalmic and Vision Research, after approval of the laboratory animal protocol by the University Committee on Use and Care of Animals (UCUCA) of the University of Michigan (Protocol PRO00006486, PI Yannis Paulus).

1. System configuration

1. Photoacoustic microscopy (PAM)
    1. Use an optical parametric oscillator (OPO) laser pumped by a diode-pumped solid-state laser as the light source of the PAM. Select proper technical specifications, such as pulse repetition rate 1 kHz, pulse duration 3 - 6 ns, and tunable wavelength range 405 - 2600 nm.
    2. Reflect the emanating beam from the laser at 570 nm by two mirrors (M1 and M2), then pass it through a half-wave plate attenuator mounted on a motorized rotation stage, and finally focus, filter, and collimate it by a beam collimator (**Figure 1**). Optimize the design of the beam collimator. An example configuration of the beam collimator includes a focusing lens L1 (focal length 250 mm), a pinhole (diameter 50 μm), and a collimating lens L2 (focal length 30 mm).
    3. Divide the collimated beam by a beam splitter (BS1) with a split ratio of 90/10 (reflection/transmission). Record the transmitted portion by a photodiode for pulse-to-pulse laser energy monitoring. Successively deflect the reflected portion by a mirror (M3) and a dichroic mirror (DM) and raster-scan it using a two-dimensional galvanometer. The galvanometer is a shared component with the spectral domain (SD)-OCT system (described below).
    4. Deliver the scanned beam through a telescope composed of a scan lens (focal length 36 mm) and an ophthalmic lens (OL, focal length 10 mm) and finally focus it on the fundus by the rabbit eye optics.
    5. Select a needle-shaped ultrasonic transducer with proper technical specifications, for example, center frequency 27 MHz, two-way −6 dB bandwidth 60%. Place it in contact with the conjunctiva off the central visual axis to capture excited photoacoustic signal.
    6. Amplify the signal using an ultrasonic amplifier (for example, gain 57 dB), filter it by a low-pass filter (for example, cutoff frequency 32 MHz), and digitize it by a high-speed digitizer at a sampling rate of 200 MS/s.
    7. Place a power meter above the rabbit eye and measure the laser pulse energy on the rabbit cornea to keep it below the ANSI safety limit 160 nJ at 570 nm[38]. Block the beam to avoid laser overexposure using a laser shutter controlled from Matlab through a synchronization electronics.
    8. Synchronize the laser, the galvanometer, and the digitizer through a data acquisition (DAQ) board. Program the software for system control and data acquisition in Matlab.

2. Spectral-domain optical coherence tomography (SD-OCT)
    1. Adapt the SD-OCT system based on a commercially available system by adding an ophthalmic lens (OL) after the scan lens (SL) and a piece of dispersion compensation glass (DCG) in the reference arm (**Figure 1**). The modification enables that the OCT system can image the posterior segment of the rabbit eye.
    2. Use a zooming housing tube to adjust the length of the reference arm to ensure its match with the optical path length of the sample arm. Use an iris to control the intensity of retro-reflected reference light to ensure its match with back-scattered light intensity from the rabbit fundus to achieve maximum image contrast.
    3. Employ a charge-coupled device (CCD) camera encapsulated in the scan head for real-time visualization of rabbit fundus with an illumination light emitting diode (LED) as an external illumination source.

2. System alignment

1. Initialize the position of the galvanometer and align the OCT system by adjusting the screws of the fiber collimator mount and the beamsplitter cube.
   NOTE: The step-by-step procedures are available in the manual of the commercially acquired OCT system and will not be covered here. This step is mainly to ensure correct alignments of the fiber collimator, the reference arm, and the scan lens to maximize the performance of the OCT system.
2. Adjust the *x*, *y*, and *z* position of the pinhole around the focus of the focusing lens to spatially filter out the laser beam and maximally transmit laser energy. Check the heights of the laser beam before and after the pinhole using a height measurement tool to ensure that they are the same.
3. Adjust the tilt, decenter, and *z* position of the collimating lens L2 to collimate the filtered beam. Ensure that the beam has approximately the same size and height when observed in the near field and the far field.
4. Co-axially combine the PAM laser beam and the OCT light beam by tuning the tilts of the mirror and the DM. After this step, the PAM laser and OCT light should be fully coincident and scanning regions on the rabbit fundus are the same.
5. Adjust the tilt and decenter of the OL lens to correctly align it in the optical path. Once done, the dual-modality system is ready for imaging.
   NOTE: One can use the auto-collimation method to achieve this, i.e., checking the light back-reflected by the OL lens surface to make sure that it goes back along the same way as the incident light.

3. Rabbit preparation

1. Take a New Zealand White rabbit from the animal facility and record individual information, such as body weight and animal number.
2. Mount rabbit platforms, including the body support and the head support on the optical table below the imaging system. Put a water-circulating heating blanket on the body support and set the temperature of the circulating water to 38 °C to help keep the body temperature of the rabbit warm for the duration of the experiment and recovery.
3. Record the pre-procedure vitals, including overall animal state, mucous membrane color, heart rate, respiratory rate, and rectal body temperature. Anesthetize the rabbit with a mixture of ketamine (40 mg/kg) and xylazine (5 mg/kg) through intramuscular (IM) injection and record the usage of ketamine (Schedule III controlled substance). Confirm the anesthesia level by checking its heart rate, respiratory rate, and overall state.
4. Dilate the rabbit pupils using one drop each of Tropicamide 1% ophthalmic and phenylephrine hydrochloride 2.5% ophthalmic.
5. Use a speculum to hold the eyelids out of the way and apply a drop of eye lubricant to moisten the cornea. Instill a drop of topical Tetracaine 0.5% in the eye before the imaging procedure.
   NOTE: For longer procedures or procedures with possible discomfort to the animal, give the rabbit a subcutaneous injection of meloxicam before the experiment to ensure animal comfort.

4. SD-OCT imaging

1. Transfer the rabbit to the imaging platform of a clinical fundus camera and take 50 degree fundus, red free, and autofluorescence images before the OCT imaging session. This helps check optical transparency of the eye and recognize fundus vessel morphology and landmarks, such as the optic nerve and medullary ray retinal vasculature.
2. Transfer the rabbit to the platform of the OCT system and adjust its posture to roughly position one of the eyes under the OL. Illuminate the eye using the LED light.
   Note: To facilitate the clinical translation of the technique, the rabbit eyes are not stabilized using any other methods and the rabbit head is just put on the head support without any fixation.
3. Open the OCT software and first check the CCD camera image of the fundus. Finely adjust the height and angle of the head support if necessary to ensure region of interests (ROIs), such as choroidal vessels and retinal vessels, are within the field of view (FOV) of the camera.
   Note: If the rabbit is under a good anesthesia level, one sequential imaging session can last as long as 10 min without the need of re-adjusting the rabbit head.
4. Draw a straight line to represent the OCT B-scan of interest and start scanning. Adjust the reference arm length to visualize the OCT image and optimize the dispersion compensation factor in the OCT software to get the sharpest images.
   Note: When adjusting the reference arm length, two mirrored OCT images will appear one after the other. The correct image could be distinguished based on prior knowledge of the fundus anatomy.
5. Set data acquisition parameters, such as number of pixels and averages, and save images.
6. Observe the respiratory rate and heart rate of the rabbit to estimate the anesthesia level and animal comfort. For longer sessions, a one third dose of supplemental ketamine or inhaled isoflurane could be considered with endotracheal intubation, a V-gel, or a face mask to maintain the plane of anesthesia when necessary.
7. Rinse the rabbit cornea with eyewash every 2 min during the experiment to prevent corneal surface dehydration and corneal superficial punctate epithelial keratopathy. Monitor and record animal vitals every 15 min.

5. PAM imaging

1. Wear appropriate laser safety goggles and turn on the OPO laser.
2. Start the PAM control software, tune the laser wavelength to one of the absorption peaks of the targeted chromophores (*e.g.,* 570 nm for hemoglobin), initialize the position of the galvanometer, and monitor laser energy before the rabbit cornea to ensure that it is below the ANSI safety limit.
3. Mount the ultrasonic transducer on a three-dimensional (3D) translation stage and position the transducer tip in contact with the rabbit conjunctiva pointing to the fundus. Use a drop of eye lubricant to better couple the transducer tip and rabbit conjunctiva.
4. Turn on the LED illumination light and visualize the rabbit fundus through the Matlab software.
5. Set the scanning ROI (either retinal vessels or choroidal vessels), including the center and the physical size. Open the laser shutter and start B-scan of the beam. By roughly align the transducer, one should be able to see detected photoacoustic signal on the oscilloscope. If not, slightly adjust the eye position to scan a different region of the cornea or switch to the other eye and repeat the above processes.
6. Observe the detected photoacoustic signal on the oscilloscope and finely tune the transducer position to maximize signal intensity along the entire B-scan.
   Note: Due to limited beam width, ultrasonic transducer usually has a small FOV[41]. This step determines the background modulation of final PAM images. Misalignment will lead to PAM images with heterogeneous background and degrade image quality greatly.
7. Set data acquisition parameters. This includes the number of pixels (*e.g.*, 256×256 pixels), sampling rate (*e.g.*, 200 MS/s), and delay time. Start data acquisition. The Matlab software will automatically open the shutter to pass the laser beam when started and close the shutter to block the beam when finished to avoid laser overexposure.
   Note: Limited by the pulse repetition rate (1 kHz) of the laser, it takes about 1 min to finish the data acquisition of an image with 256 × 256 pixels.
8. Process the raw data and visualize the PAM image in two dimensions (2D) through maximum intensity projection (MIP)[13] or in 3D through volumetric rendering[38].
9. Unmount the ultrasonic transducer, rinse the tip using deionized water, and put it back to the storage case.
10. Transfer the rabbit to the fundus camera and re-examine the fundus. This step helps to check whether there are any morphological changes of the fundus after the imaging session.

11. Rinse the rabbit cornea with eyewash every two min during the experiment to prevent corneal surface dehydration and keratopathy. Monitor and record animal vitals every 15 min.
    Note: The PAM, OCT, and fundus imaging sessions take approximately 1 h.

6. Post imaging

1. After fundus re-examination using the fundus camera, disconnect the V-gel if connected. Rinse the eye using eyewash, apply flurbiprofen ophthalmic and neomycin and polymyxin B sulfates and dexamethasone ophthalmic ointment, and close the eye.
2. Transfer the rabbit with the water-circulating blanket to a recover chamber. Shield the box from light and wait until the rabbit naturally wakes up. During this period, monitor animal vitals every 15 min and keep the record and return a copy to the animal facility for recordkeeping.
3. Once the rabbit wakes up and is active, alert and walking normally, transport it back to the animal facility. If an acute experiment is planned, euthanize the animal using euthanasia solution (*e.g.*, Beuthanasia, 0.22 mL/kg, intravenous injection in the marginal ear vein) and dispose of the carcass.
4. Turn off the software and the laser. Clean the optical bench.

Representative Results

The dual-modality imaging system and experimental protocol have been successfully tested in the authors' laboratory using four New Zealand White rabbits. The following showcases some representative results.

Figure 1 shows the schematic of the PAM and SD-OCT dual-modality imaging system. It is composed of the following modules: photoacoustic light source, variable laser attenuator, beam collimator, energy meter, scan head, photoacoustic detection and acquisition module, OCT unit, and synchronization electronics. Detailed system configurations are itemized in Section 1.1.

Figure 2 demonstrates typical imaging results of rabbit choroidal vasculature acquired using the dual-modality imaging system. **Figure 2(a)** is a fundus photograph showing that choroidal vessels spread over most parts of the rabbit fundus while retinal vessels are confined within the medullary ray. **Figure 2(b)** is a typical PAM image showing the choroidal vasculature within the fundus photograph. The choroidal blood vessels were delineated at high lateral resolution. **Figure 2(c)** is an OCT B-scan image acquired to look at the fundus anatomy and confirms the presence of the choroidal vessels. The retina, the choroid, and the sclera could be visualized with a high axial resolution with the choroidal vessels below the retinal pigment epithelium (RPE) layer.

Figure 3 demonstrates typical imaging results of rabbit retinal vasculature acquired using the dual-modality imaging system. **Figures 3(a)** and **3(b)** are 2D MIP and 3D volumetric rendering of retinal vessels obtained by PAM, respectively. **Figure 3(c)** shows orthogonal slices of the 3D image. The results show that the PAM could also visualize individual retinal vessels, which lie above the RPE layer, and confirms that retinal vessels and choroidal vessels are at different depths. **Figure 3(d)** illustrates a corresponding OCT B-scan image, showing cross sections of individual retinal vessels and the nerve fiber layer (NFL).

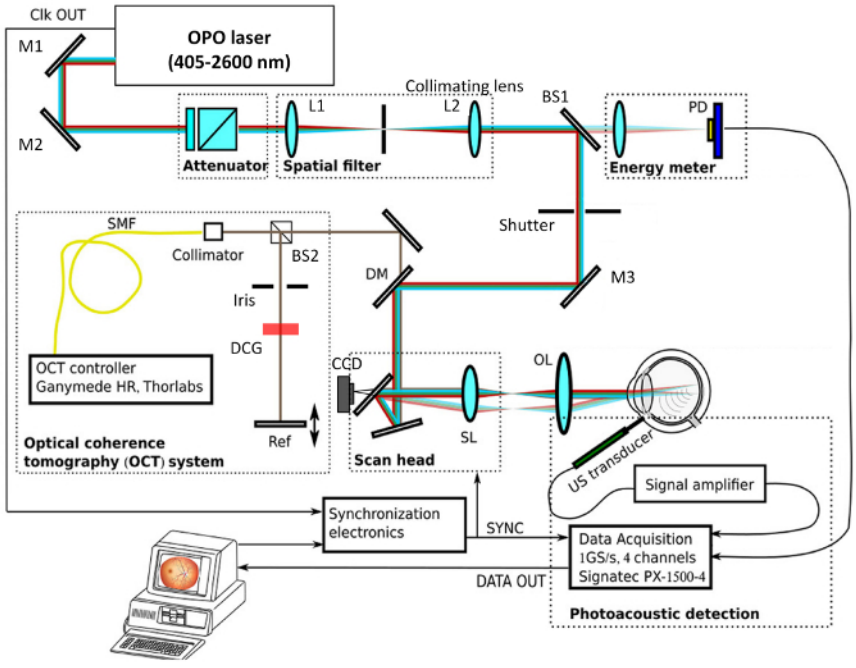

Figure 1.Schematic of the integrated photoacoustic microscopy and optical coherence tomography dual-modality imaging system. OPO: Optical parametric oscillator; BS: beam splitter; PD: photodiode; M: Mirror; DM: dichroic mirror; SL: scan lens; OL: ophthalmic lens; SMF: single-mode fiber; DCG: dispersion compensation glass; CCD: charge-coupled device. Please click here to view a larger version of this figure.

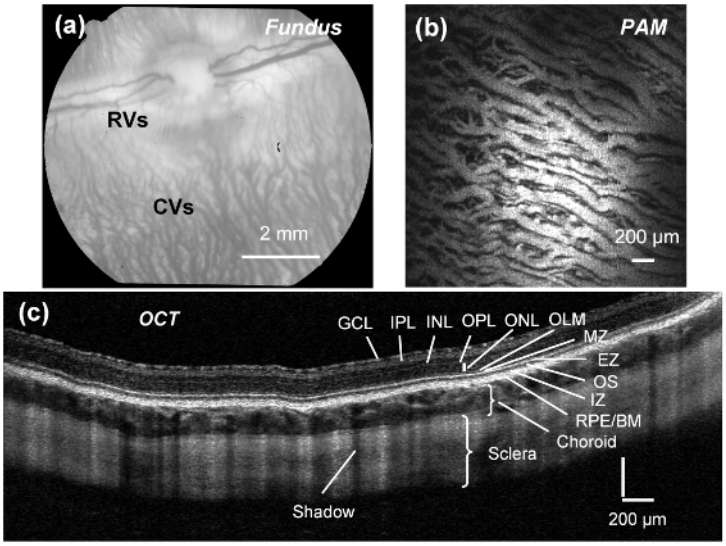

Figure 2. **PAM and OCT dual-modality imaging of choroidal blood vessels in rabbits.** (a) Fundus photograph showing that choroidal vessels (CVs) spread over the entire fundus while retinal vessels (RVs) are confined within the medullary ray since rabbits are merangiotic animals. (b) PAM C-scan image of CVs showing that PAM can delineate CVs at high lateral resolution. (c) OCT B-scan image showing the anatomical structure of rabbit fundus and axial position of choroidal vessels. GCL: Ganglion cell layer; INL: inner nuclear layer; IPL: inner plexiform layer; ONL: outer nuclear layer; OPL: outer plexiform layer; OLM: outer limiting membrane; EZ: ellipsoid zone; MZ: myoid zone; OS: outer segment; BM, Bruch's membrane; IZ: interdigitation zone[38]. Please click here to view a larger version of this figure.

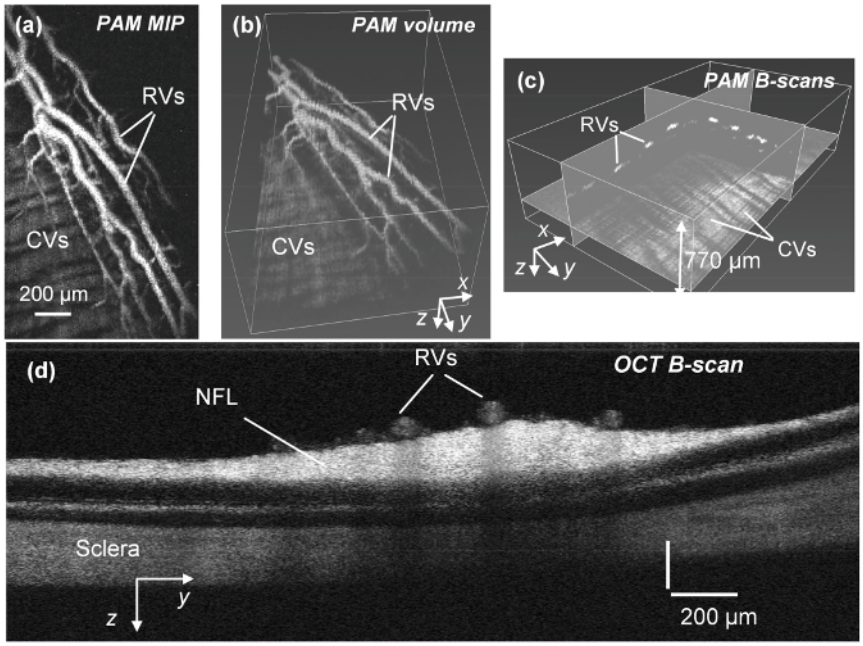

Figure 3. **PAM and OCT dual-modality imaging of retinal blood vessels in rabbits.** (a) PAM C-scan image of RVs and CVs. (b) 3D volumetric rendering of the PAM image. (c) 2D orthogonal slices of the PAM image showing that RVs and CVs are at different depths. (d) OCT B-scan image illustrating the RVs, the NFL, and the sclera[38]. Please click here to view a larger version of this figure.

Discussion

An intact and regular tear film is essential for high-quality fundus images. An irregular and deteriorated tear films can significantly degrade image quality[42]. To preserve the integrity of the tear film and prevent corneal superficial punctate keratopathy, it is critical to lubricate the cornea using eyewash very frequently, approximately every two min. If there are any concerns regarding the opacity of the eye, use a slit lamp and fluorescein strips to check the cornea conditions.

Several difficulties may be present for posterior segment imaging of the eyes of larger animals, including photoacoustic signal attenuation with distance particularly for high-frequency components, corneal dehydration, and optical aberrations. Photoacoustic signal amplitude typically experiences significant attenuation before being detected by the needle-shaped ultrasonic transducer. The larger the eyeball size, the greater the attenuation. The eyeball size of rabbits (~18.1mm) is about three times larger than that of rats and six times larger than that of mice, which makes rabbit eye imaging particularly challenging. To achieve reasonable imaging quality, a laser beam with a small diameter (2 mm after the beam collimator in this study) and collimated wavefront (ideally planar wavefront) is preferred because it will be minimally affected by intrinsic optical aberrations of the cornea and can be well focused onto the retina. This point is of critical importance in terms of reducing the laser exposure dose and improving image resolution. In addition, an ultrasonic transducer with a center frequency of 27 MHz rather than a higher center frequency due to experimental results indicating that this is the maximal ultrasound signal at this distance.

While OCT and OCTA are well-established technologies used in the clinic for anatomical and functional imaging of the eye, their molecular imaging capability is limited due to the contrast mechanisms[43]. PAM is an emerging eye imaging modality based on optical absorption contrast of ocular tissue. It is sensitive to endogenous and exogenous chromophores, like hemoglobin, melanin, and externally-administrated contrast agents. Visualizing vascular structure demonstrated in this work is one of the many applications of PAM. Other important applications include functional and molecular imaging, such as blood flow speed detection, hemoglobin concentration quantification, oxygen saturation mapping, and biomarker visualization, which are important to study the pathophysiology of a myriad of retinal vascular diseases, including diabetic retinopathy, macular degeneration, retinal vein occlusions, retinal artery occlusions, sickle cell retinopathy, and presumed ocular histoplasmosis, to name a few. Moreover, PAM has greater penetration depth than OCT, which makes it suitable for the study of some choroidal diseases, such as polypoidal choroidal vasculopathy, central serous chorioretinopathy, pachychoroid diseases, and choroidal neovascularization. From these perspectives, PAM might be able to provide useful complementary information to OCT and OCTA to give a more comprehensive evaluation of ocular diseases in the future.

Disclosures

The authors have nothing to disclose.

Acknowledgements

This work was supported by the generous support of the National Eye Institute 4K12EY022299 (YMP), Fight for Sight-International Retinal Research Foundation FFS GIA16002 (YMP), unrestricted departmental support from Research to Prevent Blindness, and the University of Michigan Department of Ophthalmology and Visual Sciences. This work utilized the Core Center for Vision Research funded by P30 EY007003 from the National Eye Institute.

References

1. Wang, L. V., Hu, S. Photoacoustic tomography: in vivo imaging from organelles to organs. *Science.* **335** (6075), 1458-1462 (2012).
2. Beard, P. Biomedical photoacoustic imaging. *Interface Focus.* rsfs20110028 (2011).
3. Taruttis, A., Ntziachristos, V. Advances in real-time multispectral optoacoustic imaging and its applications. *Nat Photonics.* **9** (4), 219-227 (2015).
4. Tian, C., Xie, Z., Fabiilli, M. L., Wang, X. Imaging and sensing based on dual-pulse nonlinear photoacoustic contrast: a preliminary study on fatty liver. *Opt Lett.* **40** (10), 2253-2256 (2015).
5. Tian, C. *et al.* Dual-pulse nonlinear photoacoustic technique: a practical investigation. *Biomed Opt Express.* **6** (8), 2923-2933 (2015).
6. Tian, C. *et al.* Non-Contact Photoacoustic Imaging Using a Commercial Heterodyne Interferometer. *IEEE Sens J.* **16** (23), 8381-8388 (2016).
7. Kim, K. H. *et al.* Air-coupled ultrasound detection using capillary-based optical ring resonators. *Sci Rep.* **7** 1 (2017).
8. Feng, T. *et al.* Bone assessment via thermal photo-acoustic measurements. *Opt Lett.* **40** (8), 1721-1724 (2015).
9. Chen, S.-L., Xie, Z., Carson, P. L., Wang, X., Guo, L. J. In vivo flow speed measurement of capillaries by photoacoustic correlation spectroscopy. *Opt Lett.* **36** (20), 4017-4019 (2011).
10. De, n-Ben, X., Fehm, T. F., Razansky, D. Universal Hand-held Three-dimensional Optoacoustic Imaging Probe for Deep Tissue Human Angiography and Functional Preclinical Studies in Real Time. *J Vis Exp.* (93), e51864 (2014).
11. Galanzha, E. I. *et al.* In vivo magnetic enrichment and multiplex photoacoustic detection of circulating tumour cells. *Nat Nanotechnol.* **4** (12), 855-860 (2009).
12. Xiang, L., Wang, B., Ji, L., Jiang, H. 4-D photoacoustic tomography. *Sci Rep.* **3** (2013).
13. Tian, C. *et al.* Plasmonic nanoparticles with quantitatively controlled bioconjugation for photoacoustic imaging of live cancer cells. *Adv Sci.* **3** (12) (2016).
14. Zhou, F., Wu, S., Yuan, Y., Chen, W. R., Xing, D. Mitochondria-Targeting Photoacoustic Therapy Using Single-Walled Carbon Nanotubes. *Small.* **8** (10), 1543-1550 (2012).
15. Maslov, K., Zhang, H. F., Hu, S., Wang, L. V. Optical-resolution photoacoustic microscopy for in vivo imaging of single capillaries. *Opt Lett.* **33** (9), 929-931 (2008).
16. Hu, S., Maslov, K., Wang, L. V. Three-dimensional Optical-resolution Photoacoustic Microscopy. *J Vis Exp.* (51), e2729 (2011).
17. Yao, J. *et al.* High-speed label-free functional photoacoustic microscopy of mouse brain in action. *Nat Methods.* **12** (5), 407-410 (2015).
18. Yang, X., Skrabalak, S. E., Li, Z.-Y., Xia, Y., Wang, L. V. Photoacoustic tomography of a rat cerebral cortex in vivo with au nanocages as an optical contrast agent. *Nano Lett.* **7** (12), 3798-3802 (2007).
19. Agarwal, A. *et al.* Targeted gold nanorod contrast agent for prostate cancer detection by photoacoustic imaging. *J Appl Phys.* **102** (6), 064701 (2007).
20. Zackrisson, S., van de Ven, S., Gambhir, S. Light in and sound out: emerging translational strategies for photoacoustic imaging. *Cancer Res.* **74** (4), 979-1004 (2014).
21. Ermilov, S. A. *et al.* Laser optoacoustic imaging system for detection of breast cancer. *J Biomed Opt.* **14** (2), 024007 (2009).

22. Mallidi, S., Luke, G. P., Emelianov, S. Photoacoustic imaging in cancer detection, diagnosis, and treatment guidance. *Trends Biotechnol.* **29** (5), 213-221 (2011).
23. Zhang, H. F., Maslov, K., Stoica, G., Wang, L. V. Functional photoacoustic microscopy for high-resolution and noninvasive in vivo imaging. *Nat Biotechnol.* **24** (7), 848 (2006).
24. Keswani, R. K. *et al.* Repositioning Clofazimine as a Macrophage-Targeting Photoacoustic Contrast Agent. *Sci Rep.* **6** 23528 (2016).
25. Strohm, E. M., Berndl, E. S., Kolios, M. C. Probing red blood cell morphology using high-frequency photoacoustics. *Biophys J.* **105** (1), 59-67 (2013).
26. Nguyen, V. P., Kim, J., Ha, K.-I., Oh, J., Kang, H. W. Feasibility study on photoacoustic guidance for high-intensity focused ultrasound-induced hemostasis. *J Biomed Opt.* **19** (10), 105010 (2014).
27. Keane, P. A., Sadda, S. R. Retinal imaging in the twenty-first century: state of the art and future directions. *Ophthalmology.* **121** (12), 2489-2500 (2014).
28. Keane, P., Sadda, S. Imaging chorioretinal vascular disease. *Eye.* **24** (3), 422-427 (2010).
29. Jiao, S. *et al.* Photoacoustic ophthalmoscopy for in vivo retinal imaging. *Opt Express.* **18** (4), 3967-3972 (2010).
30. Liu, T. *et al.* Near-infrared light photoacoustic ophthalmoscopy. *Biomed Opt Express.* **3** (4), 792-799 (2012).
31. Song, W. *et al.* A combined method to quantify the retinal metabolic rate of oxygen using photoacoustic ophthalmoscopy and optical coherence tomography. *Sci Rep.* **4** 6525 (2014).
32. Liu, W., Zhang, H. F. Photoacoustic imaging of the eye: a mini review. *Photoacoustics.* **4** (3), 112-123 (2016).
33. La Zerda, A. *et al.* Photoacoustic ocular imaging. *Opt Lett.* **35** (3), 270-272 (2010).
34. Hu, S., Rao, B., Maslov, K., Wang, L. V. Label-free photoacoustic ophthalmic angiography. *Opt Lett.* **35** (1), 1-3 (2010).
35. Silverman, R. H. *et al.* High-resolution photoacoustic imaging of ocular tissues. *Ultrasound Med Biol.* **36** (5), 733-742 (2010).
36. Wu, N., Ye, S., Ren, Q., Li, C. High-resolution dual-modality photoacoustic ocular imaging. *Opt Lett.* **39** (8), 2451-2454 (2014).
37. Hennen, S. N. *et al.* Photoacoustic tomography imaging and estimation of oxygen saturation of hemoglobin in ocular tissue of rabbits. *Exp Eye Res.* **138** 153-158 (2015).
38. Tian, C., Zhang, W., Mordovanakis, A., Wang, X., Paulus, Y. M. Noninvasive chorioretinal imaging in living rabbits using integrated photoacoustic microscopy and optical coherence tomography. *Opt Express.* **25** (14), 15947-15955 (2017).
39. Laser Institute of America. *American National Standard for Safe Use of Lasers ANSI Z136.1 - 2007.* American National Standards Institute, Inc., (2007).
40. Hughes, A. A schematic eye for the rabbit. *Vision Res.* **12** (1), 123-IN126 (1972).
41. Ma, T. *et al.* Systematic study of high-frequency ultrasonic transducer design for laser-scanning photoacoustic ophthalmoscopy. *J Biomed Opt.* **19** (1), 016015-016015 (2014).
42. Song, W., Wei, Q., Jiao, S., Zhang, H. F. Integrated photoacoustic ophthalmoscopy and spectral-domain optical coherence tomography. *J Vis Exp.* (71) (2013).
43. Mattison, S., Kim, W., Park, J., E Applegate, B. Molecular Imaging in Optical Coherence Tomography. *Curr Mol Imaging.* **3** (2), 88-105 (2014).

